VENTILATION TECHNOLOGY - RESEARCH AND APPLICATION

8th AIVC Conference, Überlingen, Federal Republic of Germany
21 - 24 September 1987

POSTER P5

THE INFLUENCE OF TEMPERATURE VARIATION ON STACK EFFECT IN HIGH-RISE BUILDINGS

K.H. Lee[1], Y. Lee[1] and H. Tanaka[2]

[1]Department of Mechanical Engineering
University of Ottawa, Ottawa, Canada, K1N 6N5

[2]Department of Civil Engineering
University of Ottawa, Ottawa, Canada, K1N 6N5

SYNOPSIS

A study has been made, both experimentally and analytically, on the characteristics of thermal performance of high-rise buildings using a simulated model building with five floors and a number of exterior openings under various temperature distributions. The effect of the temperature variation on the location of the neutral pressure level (NPL) was of particular interest of the present study. The results also show that for the prediction of thermal effect in high-rise buildings with floor partitions under a given temperature distribution, a nondimensional parameter representing the ratio of floor opening to exterior opening areas has a dominant role.

SYMBOLS

A	Area
b	Constants in Eq. (1)
D	Diameter, equivalent
f	Friction factor
g	Acceleration of gravity
H	Height of the building
K	Form loss coefficient
L	Length of the openings
P	Pressure
R	Gas constant
T	Temperature
v	Velocity
z	Height
ρ	Density

Subscripts

i	Inside
o	Outside; at z = 0
n	At z = NPL
p	Floor partition
r	Reference
w	Exterior wall
crit	Critical

1.0 INTRODUCTION

Air filtration is directly related to heat loss/gain through building enclosure or the transfer of odors, dust and other pollutants. The heat loss due to air filtration for insulated buildings of good construction in Canada is said to be from 30 to 40% of total heating requirements [1]. The safety regarding spread of fire and smoke in buildings also has significant relation to this topic [2].

The air filtration through building envelopes are influenced mainly by three factors; i.e., external wind flow, temperature difference between the inside and outside of the building and mechanical ventilation operation. The second cause is often referred to as the stack effect which has been found to be one of the two major causative factors for the pressure drop across building enclosure [3].

The profile and distribution of pressure differentials induced by thermal effect depend upon the construction, design and environment of the building such as exterior openings, floor partitions and temperature distributions. The magnitude of the stack effect in Canadian winter was found to be comparable to the wind-induced pressure at a mean speed of about 12 m/s [1] and even for one or two storey houses, its effect in winter time is known to be sufficient enough to induce significant air filtration [4].

It has been shown by both experiment and analysis [5] that the stack effect equation derived from the ideal gas equation of state for the uniform outside and inside temperature of a building is accurate for the prediction of the pressure differentials induced by the stack effect provided that the value of the neutral pressure level (NPL) is known correctly. The study also demonstrated that the existing method recommended by ASHRAE [6], applicable only for a simple case of openings at top and bottom levels with uniform outside and inside temperature, for the value of NPL is inadequate.

Reported herein are the results of an analytical and experimental study on the stack effect in a high-rise building where the internal temperature has a non-uniform distribution.

2.0 ANALYSIS

The schematic diagram of the analytical model is presented in Fig. 1. It represents a hypothetical tall building with floor partitions and external openings. The opening holes and crevices given by the elevator doors, stairways and various service shafts, etc., are first lumped together and represented by an equivalent orifice through the floor separation. The openings through the external envelope of the building, such as crevices around the windows and doors etc., are also represented by the equivalent exterior orifices. The opening areas per floor of these holes are expressed by A_p and A_w, respectively. The effect of the partitions between rooms in the same floor is not considered.

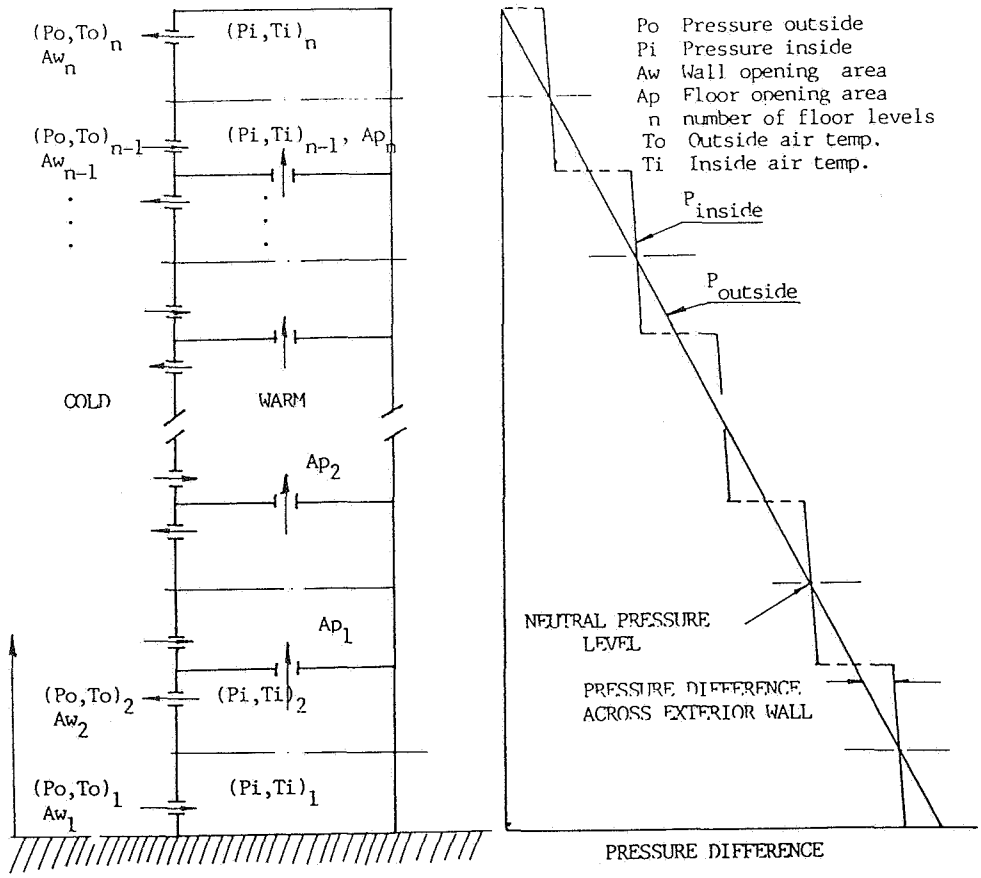

Fig. 1 Idealized Model

The major assumptions introduced for the analysis are as follows:

i. Both the inside and outside temperatures are a linear function of height as given by the following equation;

$$T_q(z) = T_q(z_r) \pm b_q z \tag{1}$$

where q = in or out,

ii. there exists no wind and mechanical ventilation actions on the building; and

iii. the flow field at the openings is steady, laminar and hydrodynamically smooth transition.

2.1 Pressure Distribution

The density difference of air between the inside and the outside caused by temperature differences across the exterior wall generates either a negative or positive inside pressure differential, depending on the magnitude of the two pressures and induces an airflow through the openings at a given elevation as illustrated in Fig. 1. The flow or pressure differentials induced by the density difference can be analyzed using the energy equation.

With Eq. (1), the governing differential equation for the pressure along the building is:

$$\left(\frac{dP}{P}\right)_q = \frac{gdz}{R[T_q(z_r) \pm b_q z]} \tag{2}$$

Integrating Eq. (2), the pressure difference due do the thermal effect between the inside and outside of the building at a given level in terms of the NPL, z_n, and the reference level, z_o (i.e., the bottom level opening), is obtained as:

$$\Delta P(z) = P_o(z_n) \left\{ \left[\frac{T_o(z_o) \pm b_o z}{T_o(z_o)} \right]^{\mp \frac{g}{b_o R}} - \left[\frac{T_o(z_o) \pm b_o z_n}{T_o(z_o)} \right]^{\mp \frac{g}{b_o R}} \left[\frac{T_i(z_o) \pm b_i z}{T_i(z_o) \pm b_i z_n} \right]^{\mp \frac{g}{b_i R}} \right\} \tag{3}$$

Eq. (3) is the basic equation for the pressure differential due to thermal effect with the temperatures distributions given by Eq. (1).

The value of NPL, z_n, may be obtained from the equations of conservation of mass and energy including the resistance, both friction and form loss, written along the flow paths of the wall openings.

2.2 Energy Equations

The energy equations representing the pressure drop across the holes are expressed as follows:

For the exterior wall openings:

$$(\Delta P)_k = (P_o - P_i)_k = \pm\ 0.5\ \rho v^2\ (f\ \frac{L}{D} + \Sigma K)_k \qquad (4)$$

where subscript k denotes the location of k-th opening, and the positive and negative signs are taken as the in-flow and out-flow openings, respectively.

For the openings at the floor partitions:

$$(\Delta P)_j = (P_i)_{j+1} - (P_i)_j = \pm\ 0.5\ \rho v^2\ (f\ \frac{L}{D} + \Sigma K)_j \qquad (5)$$

where subscript j denotes j-th floor opening. In these equations K includes all the form loss terms such as entrance loss, exit loss and losses due to bends. The friction loss coefficient, f, depends on the shape of the orifice. For the present analysis, the openings of the experimental test section are circular orifices, which can be handled by the ordinary Darcy-Weisbach expression. The crevices in actual buildings are assumed to be of rectangular shape and the corresponding friction loss is calculated using the concepts of the equivalent diameter [7].

Once the pressure drop across each opening is formulated, the mass conservation equation for each closed space is given as:

$$\Sigma(\rho v A)_{in} = \Sigma(\rho v A)_{out} \qquad (6)$$

and the equation of state for a perfect fluid make a complete package to solve the flow rate and corresponding pressure drops, ΔP, at any point across the building wall or floors.

2.3 Method of Solution

Owing to the temperature variation, the expression for the NPL is somewhat complicated and requires an iterative method.

The energy equations, Eqs. (4) and (5), corresponding to the number of exterior and interior openings in the building, are rearranged by interrelating between the openings at different levels together with Eqs. (3) and (6), and a set of equations in terms of velocities is obtained.

The total number of equations as well as the number of unknowns are identical to the number of the openings involved in the fluid flow induced by the thermal effect in the building.

Since the equations formulated include non-linear terms, the Newton's method for the solution of the set of non-linear equations [8] was used in the present study. In the method, the values for the unknowns are determined by calculating the given function with a small perturbation for each of the variables in turn, to improve the accuracy of the estimation.

The computations are initiated with assumed values for the flow velocity in the openings involved for the case under consideration. When the convergence is obtained, the next procedure to satisfy mass conservation in the system is taken.

3.0 EXPERIMENT

The purpose of the experimental program in this study is to verify the accuracy and usefulness of the analytical model described above. Therefore, the model building used in the experiment is meant not to simulate any particular building but to simulate the mechanism of stack effect in building structures. A schematic diagram of the model building simulating a high-rise building with floor partitions is presented in Fig. 2.

3.1 Description of the Test Model Building

The test section is made of 18.3 m long, vertical copper pipe with 50.8 mm ID and is equipped with 20 separate heating units along its height. Each heating unit is about 0.90 m in length and has an independent heat element which can be controlled individually. The copper pipe is thermally insulated from the ambient air. Thus, the internal temperature distribution can be given in any designed profile.

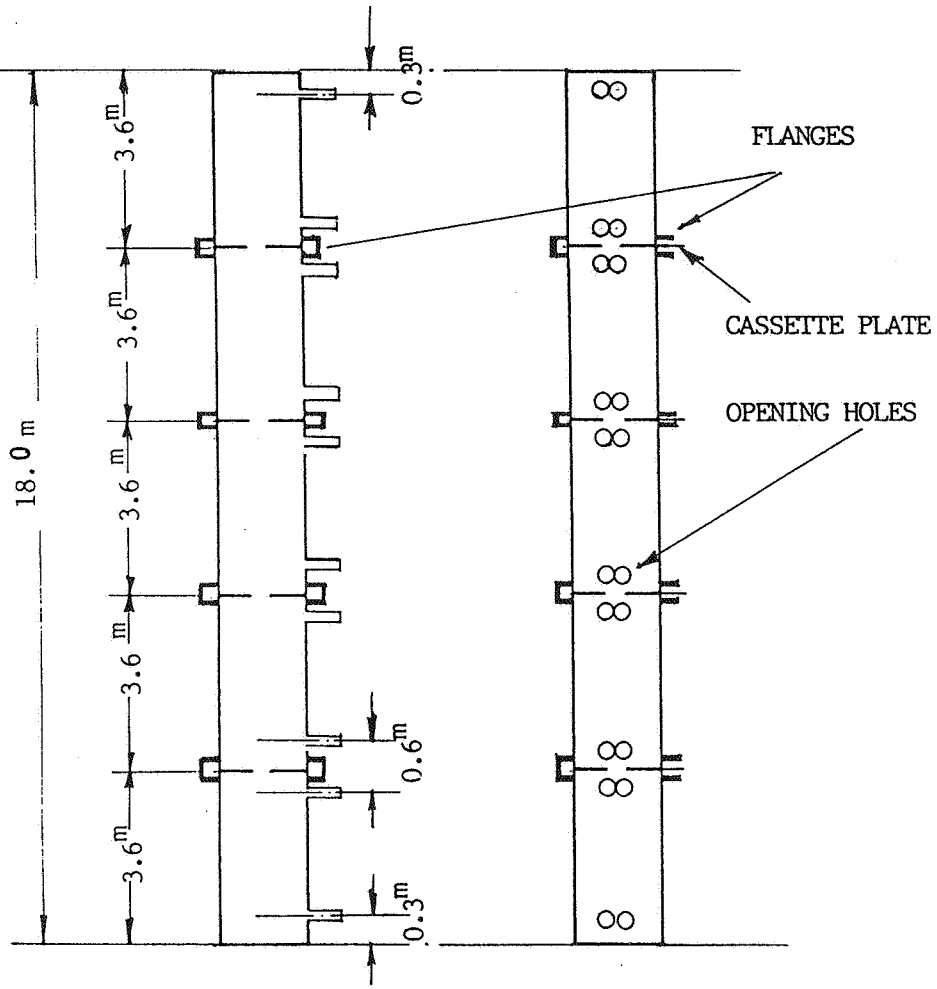

Fig. 2 Test Section with Floor Partitions

20 sets of variable transformers with 1 KW capacity, 110 V and 10 A are used to supply the power to each heating unit. The power to each heating unit is controlled by these variable transformers, and it is measured by both a digital voltmeter and an amperemeter through the measuring circuits.

38 K-type thermocouples are used in total for the measurement of temperature profiles of the test section. 20 thermocouples are spot-welded on the outer surface of the copper tube of the test section (at the center of each heating unit) to measure the wall temperatures of the test section.

In addition, 8 thermocouples were provided on the outside surface of the test section to supplement the 20 thermocouples mentioned above. 5 thermocouples, which are sheathed K-type with 152 mm long, 0.82 mm O.D stainless steel tubing, are inserted into the temperature measuring tap of the test section to measure the inside air temperature along the elevation. Another 5 were placed outside to measure the variation of the outside temperature along the test section.

Seven pressure taps were directly connected to seven sets of MKS Baratron type 220B pressure transducers with maximum pressure head of 1 torr (133 Pa), and 0.15% error at full scale. One of two pressure ports of each transducer was connected to the pressure tap of the test section and another port was connected to 17 gauge stainless steel tubes mounted immediately outside the test section at the same elevations. The signals from the pressure transducers are sent to the Data Acquisition System via a HP 3495A Scanner.

The tube is also equipped with a floor separation mechanism, which was done by inserting four cassette plates between flanges mounted on approximately every 3.6 m of the tube. The cassette plate is made of aluminum and 3.0 mm thick. The flanges are designed to allow removal and insertion of the cassette plates into flange gaps to control the air tightness of the partition as designed.

Each cassette plate has a circular hole with the diameter ranging from 1.0 to 20.0 mm at the center to simulate the porosity of the building floor separation. To simulate the external wall openings, four holes are provided for each section. Each hole is made of a copper tube of 5.0 mm ID and 75 mm long.

The height of each floor, 3.6m, is similar to the usual floor height of ordinary buildings. The cassette plate is made of aluminum and 3.0 mm thick. The flanges are designed to allow removal and insertion of the cassette plates into flange gaps to control the air tightness of the partition as designed. Each cassette plate has a circular hole at the center to simulate the crack openings of the building floor. To simulate the exterior wall openings, four holes are provided for each floor of the test section as shown in Fig. 2. Each hole is made of copper tube of 5.0 mm I.D. and 75mm long. These holes, of course, can be closed depending on the designed experimental conditions.

3.2 Data Acquisition System

The Data Acquisition System used in the present study consists of a Hewlett-Packard (HP) desk top computer with four other HP instruments as follows; HP 9835A computer, HP 3455A Digital Voltmeter, HP 3495A Scanner, HP 7245A Printer/Plotter and HP98305 Real Time Clock. The raw and reduced data are stored on magnetic tapes. Hard copies were also made available.

3.3 Experimental Procedures

The simulation of thermal effect is carried out through careful and cautious adjustment of power supply to each heating unit with continuous measurements of current and voltages supplied and the temperature distribution along the test section. This procedure is continued until the desired temperature distribution is achieved with the maximum allowable wall temperature deviation of 2 to 3 C at each point. The range of temperature difference across the wall of test section in this study is between 30 and 90 C.

4.0 RESULTS AND DISCUSSIONS

A series of experiments was carried out to confirm the validity of the above mentioned analytical model. The number of floors and the size of floor openings were varied by removing/inserting or replacing the cassette plates described in the preceding section. Since the outside air temperature was difficult to control in the experimental studies, the cases of non-uniform inside air temperatures with a uniform outside air temperature only were experimentally studied. The two linear temperature distributions used in the experiment are:

$$T(z) = 30.0 + 3.3z \quad (7)$$

$$T(z) = 90.0 - 3.3z \quad (8)$$

4.1 Thermal Effect in Building without Floor Partitions

Example of the experimental results on the thermal effect in building without floor partitions using the inside air temperature distribution represented by Eq. (7) are shown in Fig. 3 while the results obtained using those given by Eq. (8) are illustrated in Fig. 4, for various cases of external wall openings.

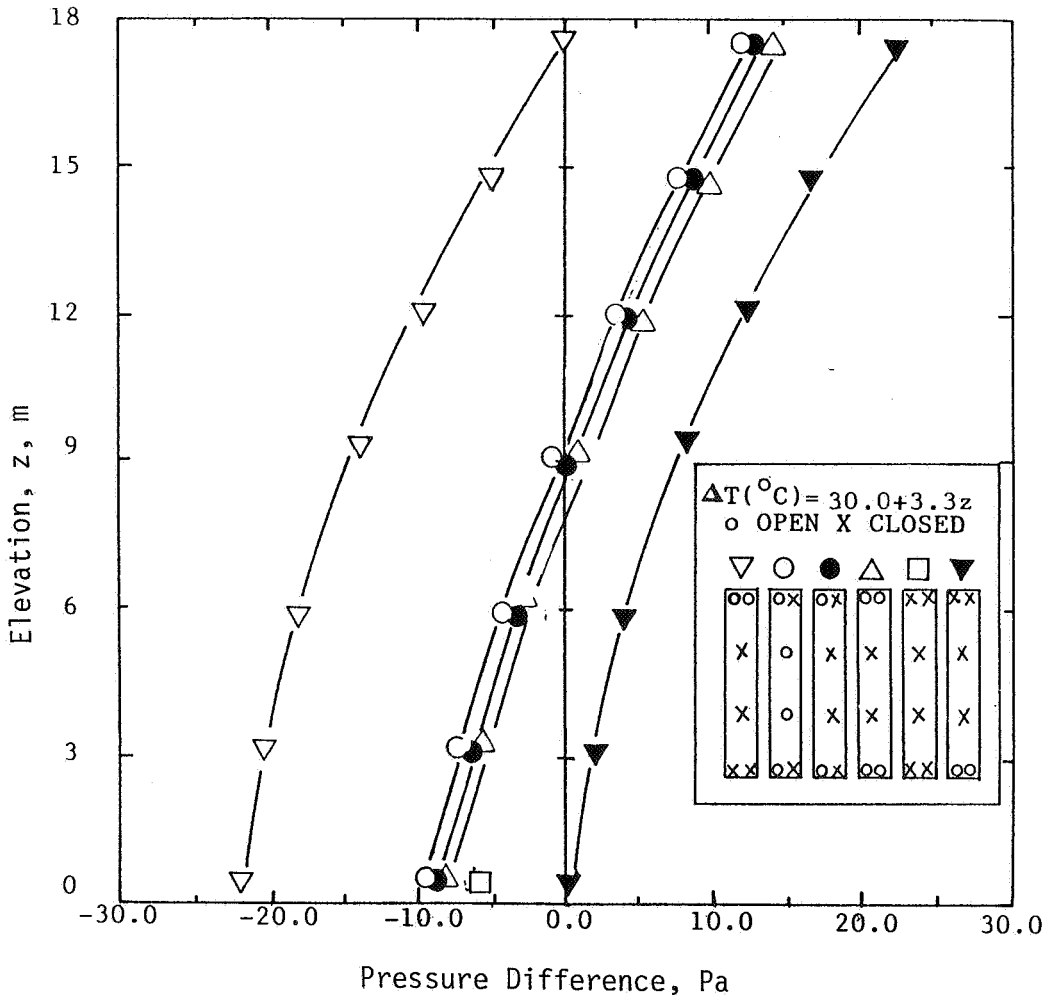

Fig. 3 Experimental Results

Figs. 5 and 6 demonstrate a comparison between the predicted and measured values. The agreement between the experiment and analysis is excellent. The results show that the location of NPL and the curvature of the pressure distribution along the height of the building are affected by the temperature distribution.

The coefficient of temperature gradient, b, is seen in Fig. 7 to have rather strong effect on the slope but very little on the location of NPL. The pressure differential across the exterior wall increases with increasing value of "b".

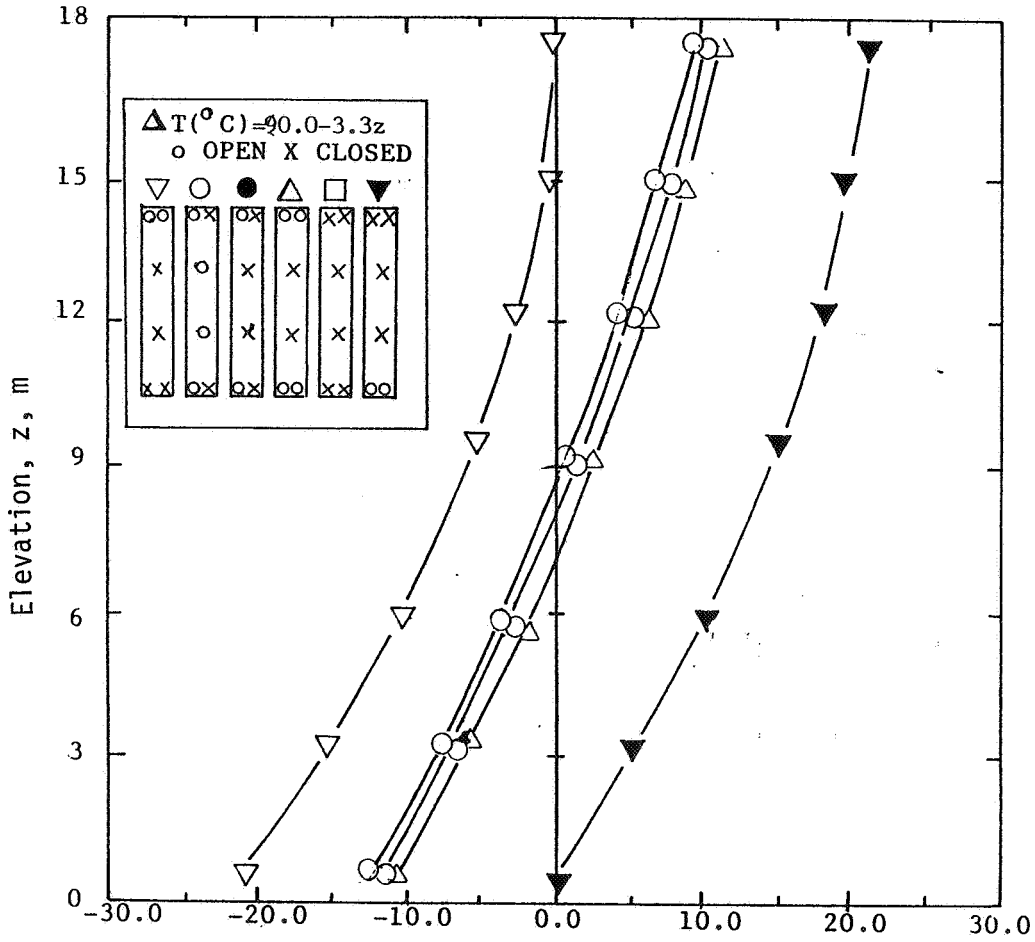

Fig. 4 Experimental Results

Fig. 8 illustrates the results of analysis on the effect of "b" with respect to the location of NPL for various cases of exterior wall openings. In all cases, the values of NPL appear to increase slightly initially as the value of "b" increases, but it becomes almost asymptotic to a constant value for $b > 0.8^{\circ}C/m$. The asymptotic values of NPL shown in Fig. 8 are about 4% higher that those obtained from the cases where the inside air temperatures were kept uniform.

4.2 Thermal Effect in Building with Floor Partitions

4.2.1 Effect of Floor Opening

Typical experimental results are shown in Fig. 9. In the figures, the vertical profiles of the pressure differentials across the building envelope are plotted for three different values of the area ratio parameter, Ap*. This parameter is defined by the ratio of the opening area in the floor partition to that of the external wall; i.e., Ap* = Ap/Aw, so that the relative magnitude of the resistance to flow imposed by the floor separations can be evaluated. The thermal boundary condition for Fig. 9 was the same as that shown in Fig. 3.

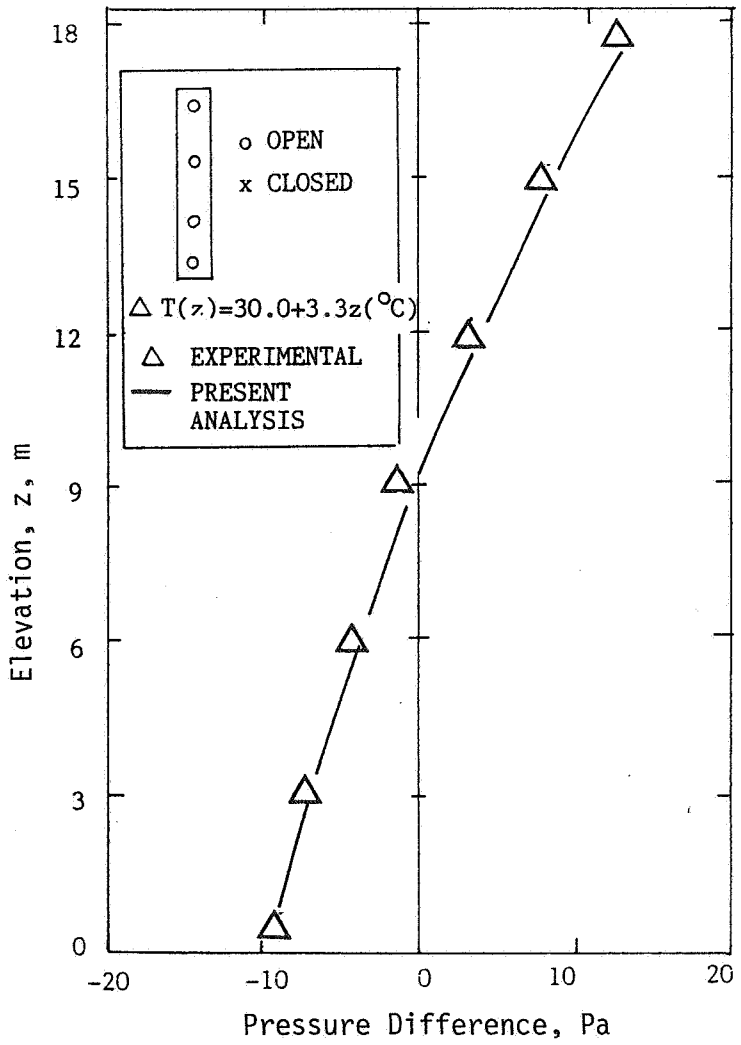

Fig. 5 Comparison of Analysis vs. Experiment

As seen in the figure, the pressure difference across floor separations decreases with increasing values of Ap*. Once it exceeds a certain value, the pressure curve along the height of the building becomes almost linear as if there were no floor partitions at all. For the cases shown in Fig. 9, the critical value of Ap* was about 8.

Also presented in the figures are the analytical results obtained from the computer model for the cases under the same conditions. It is evident that the agreement between the present analysis and the experiment is excellent in the range of the area ratio Ap* studied.

For a very small value of Ap*, as it would be expected, the pressure difference across floor partition increases significantly with the increased resistance to air flow at the openings. Correspondingly, the thermal effect in each floor appears to be less affected by other floors. Hence, it may be concluded that for the prediction of the thermal effect, it is essential to know the relative magnitude of flow resistance at the floor partitions.

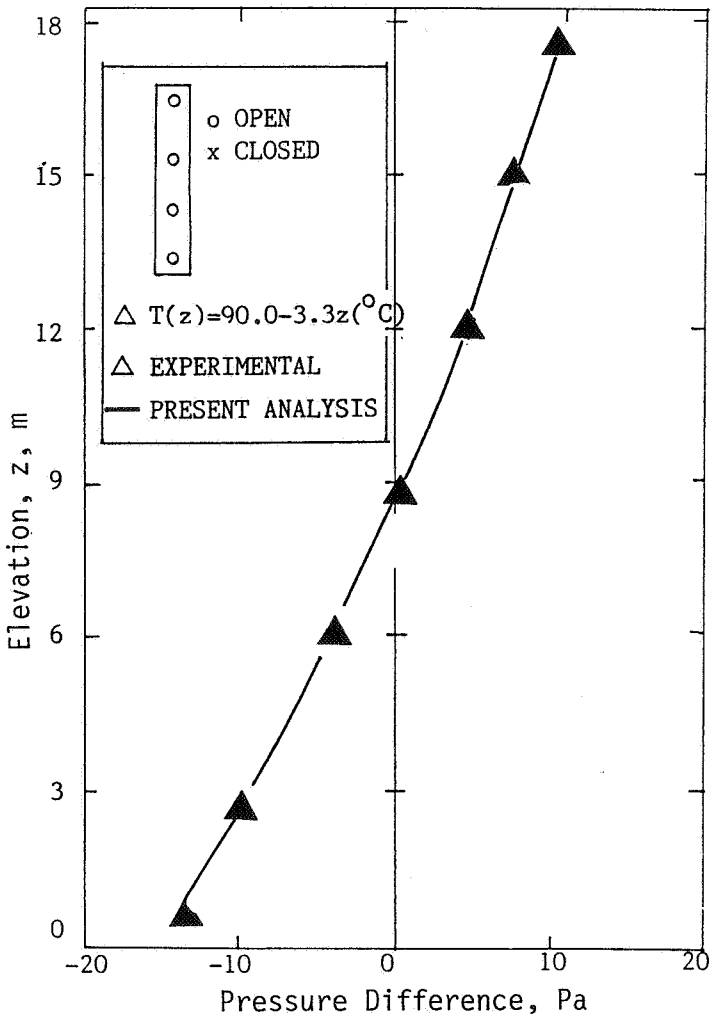

Fig. 6 Comparison of Analysis vs. Experiment

4.2.2 Critical Value of Ap*

As is obvious from Fig. 9, when the area ratio Ap* is larger than a certain value, the effect of floor separation is practically non-existent as far as the stack effect is concerned. In order to make this point clearer, the concept of the critical value of Ap* was introduced as follows [9]:

> When Ap* > (Ap*)crit, the magnitude of the pressure drop across floor partition, (Δ P)p, is less than 1 % of (ΔP)p,max, where (ΔP)p,max is the magnitude of (ΔP)p, at Ap* = 0; i.e., the case of perfectly air-tight partition.

Fig.10 represents the calculated values of (Ap*)crit defined above at a multi-story building with various

patterns of wall openings under both uniform and non-uniform inside air temperature conditions. The results for some configurations for the non-uniform inside air temperature distributions are also supported by experimental results.

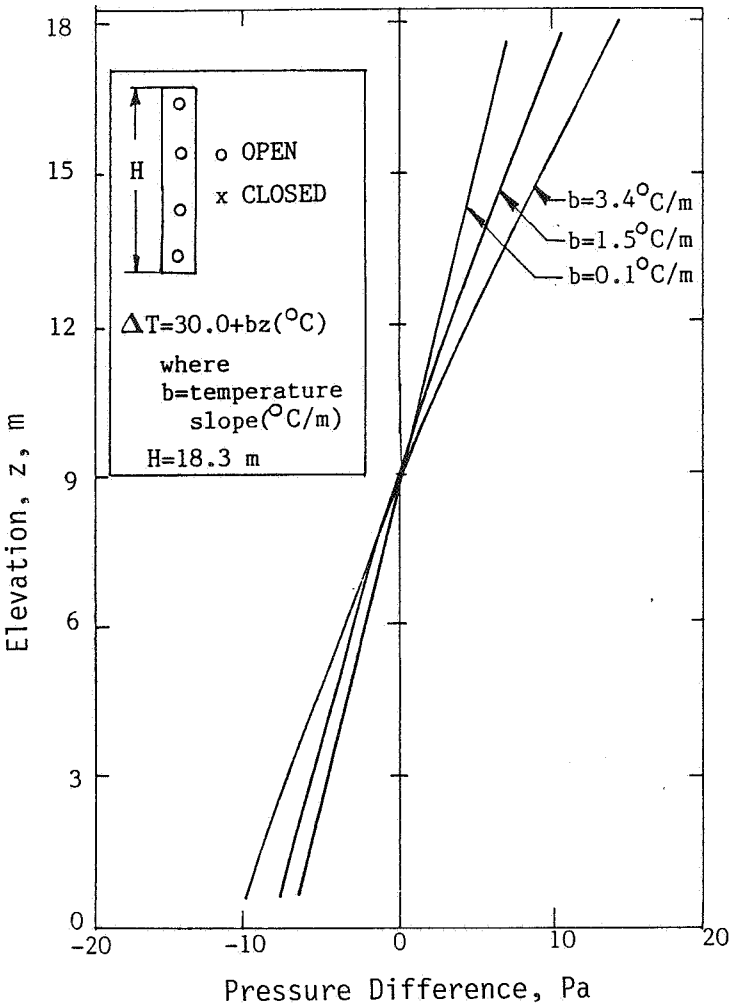

Fig. 7 Effect of "b" on Pressure Distribution

As shown in the figure, critical Ap* varies depending on the distribution of the exterior wall openings, but is found to be approximately in the range of 10 to 15 for the case of tall buildings. This is an interesting result because if the area of wall opening per each floor is typically the order of 10^{-4} m^2 for a tall building, for example, the critical value of Ap for the same building is approximately 10^{-3} m^2 per floor, which is a very much smaller value than would be expected from the door cracks of elevator shafts, stairway and various other service shafts in average construction.

Fig. 10 also illustrates that the critical value of (Ap*)crit obtained from this case appears to be nearly the same as that of the partitioned building with uniform temperature distributions. From these results, it can be deduced that the effect of the non-uniform distributions of inside air is shown to be insignificant on the critical value of (Ap*)crit.

Fig. 11 represents the effect of the temperature slope of the inside air, b, on the pressure differential profile due to the thermal effect for the different

exterior opening patterns for buildings with four floor partitions. In the analysis, the ratio of floor opening to the exterior wall opening at each floor, (Ap*), is made to be greater than (Ap*)crit in all the cases. The effect is similar to those already shown in Fig. 7 for the case of no floor partitions under non-uniform temperature distributions.

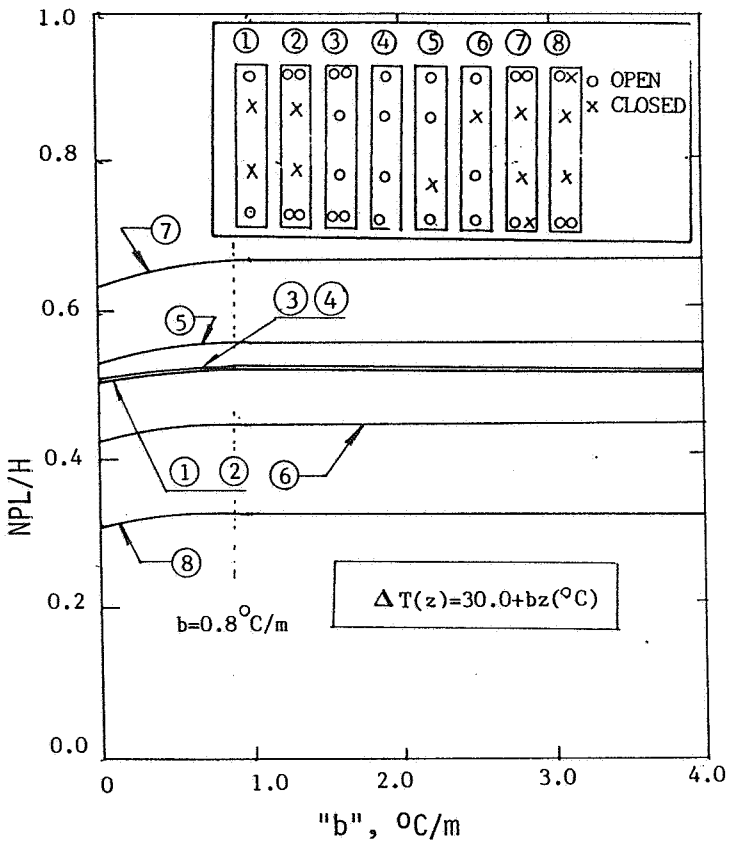

Fig. 8 Effect of "b" of Inside Air on NPL

4.2.3 Location of NPL

As was stated above, once the area ratio (Ap*) exceeds the critical value, (Ap*)crit, the behavior of thermally induced pressure differential becomes the same as that of the open shaft buildings without any internal compartmentalization. Consequently, the location of NPL becomes irrelevant to (Ap*) and is decided only by the external wall opening configuration.

The results on the effect of the temperature slope of the inside air, b, on the NPL for various distributed exterior openings are illustrated in Fig. 12. The effect is seen to be negligible as were the cases with no floor partitions shown already in Fig. 9. The values of NPL over b = 0.8 C/m are shown to be approximately 4% higher than that of the case having floor partitions with uniform temperature distribution. In practice, the effect of non-uniform temperature distributions of inside air on the neutral pressure level is marginal.

4.2.4 Effect of Both Non-Uniform Temperature Distributions of Inside and Outside Air

We have so far shown only the effects of the non-uniform temperature distributions of inside air along the height of buildings with a uniform outside air temperature, on the pressure differential profiles induced by thermal effect.

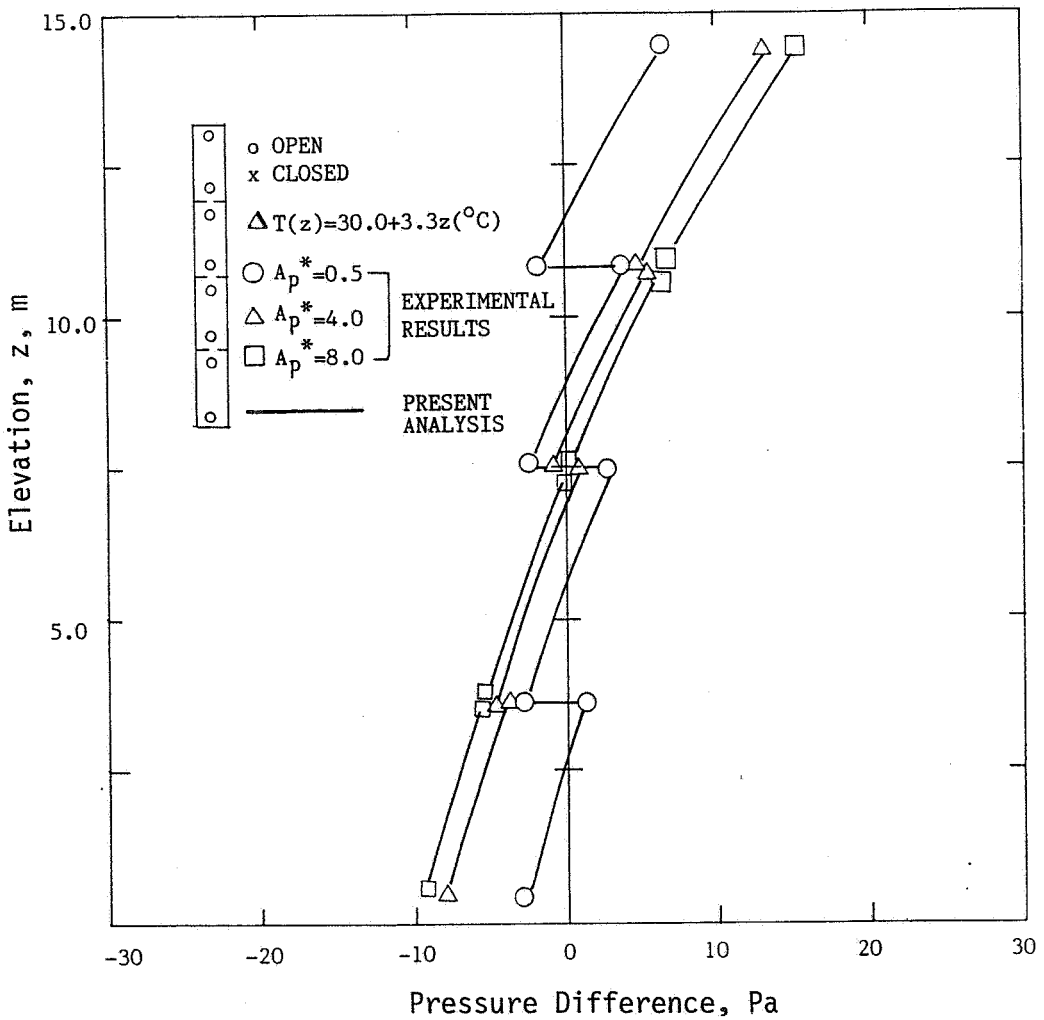

Fig. 9 Effect of Ap* on Pressure Distribution

In reality, it is quite possible that both the inside and outside air temperatures may vary along the height of buildings. Fig. 13 represents the analytical results for the case with floor partitions, in which (Ap*) is greater than (Ap*)crit. Four different temperature difference distributions along the building height are studied as shown in the figure.

It can be seen that the case of Type I which has a non-uniform temperature distributions of inside air only, is shown to have higher value of NPL/H than others.

Conversely, the case of Type IV has appeared to give lower NPL/H than others. The maximum difference between the highest and the lowest value of the NPL/H is shown to be less than 5% for the cases shown in the figure. Similar trends are also observed in other cases where exterior wall opening patterns were quite different.

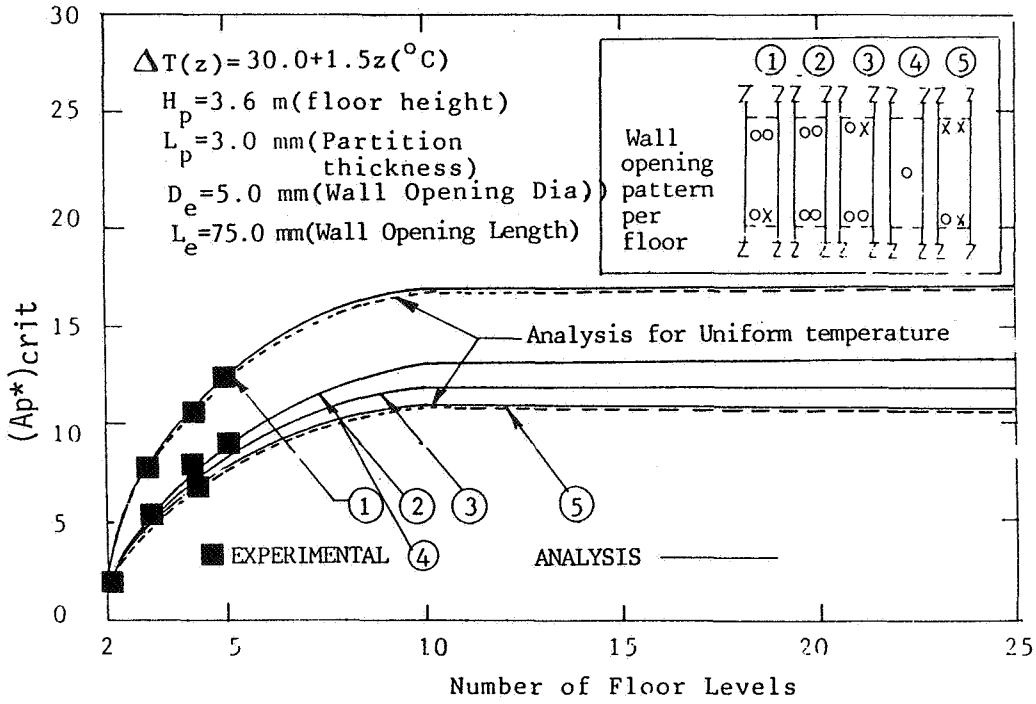

Fig. 10 Effect of Number of Floors on $(Ap^*)_{crit}$

From these results, we may conclude that the pressure differential profiles induced by the thermal effect in a building with floor separations is mainly governed by the distributed mode of the exterior wall openings as well as the openings in the floor separations including the number of floors even under the effect of the non-uniform temperature distributions of inside air along the building height.

4.3 Other Aspects of the Problem

Thus far, the floor openings and wall openings are assumed to have a shape of a simple orifice hole. Of course in reality, the cracks and crevices would have more complicated cross-sections and path shapes. Moreover, the number of holes may also have some effects on the results. These points are carefully examined here.

4.3.1 Problem of Orifice Shape

The effect of the crack opening configuration was analytically examined. The results showed that the effect of the geometrical shape of openings is not significant as was the case with a uniform temperature distribution of the inside air [9]. It can be concluded, therefore, that for the analysis of the thermal effect in buildings, the use of circular orifices with an equivalent diameter is probably a good representative of various types of cracks in actual buildings, provided that the equivalent diameter is properly decided.

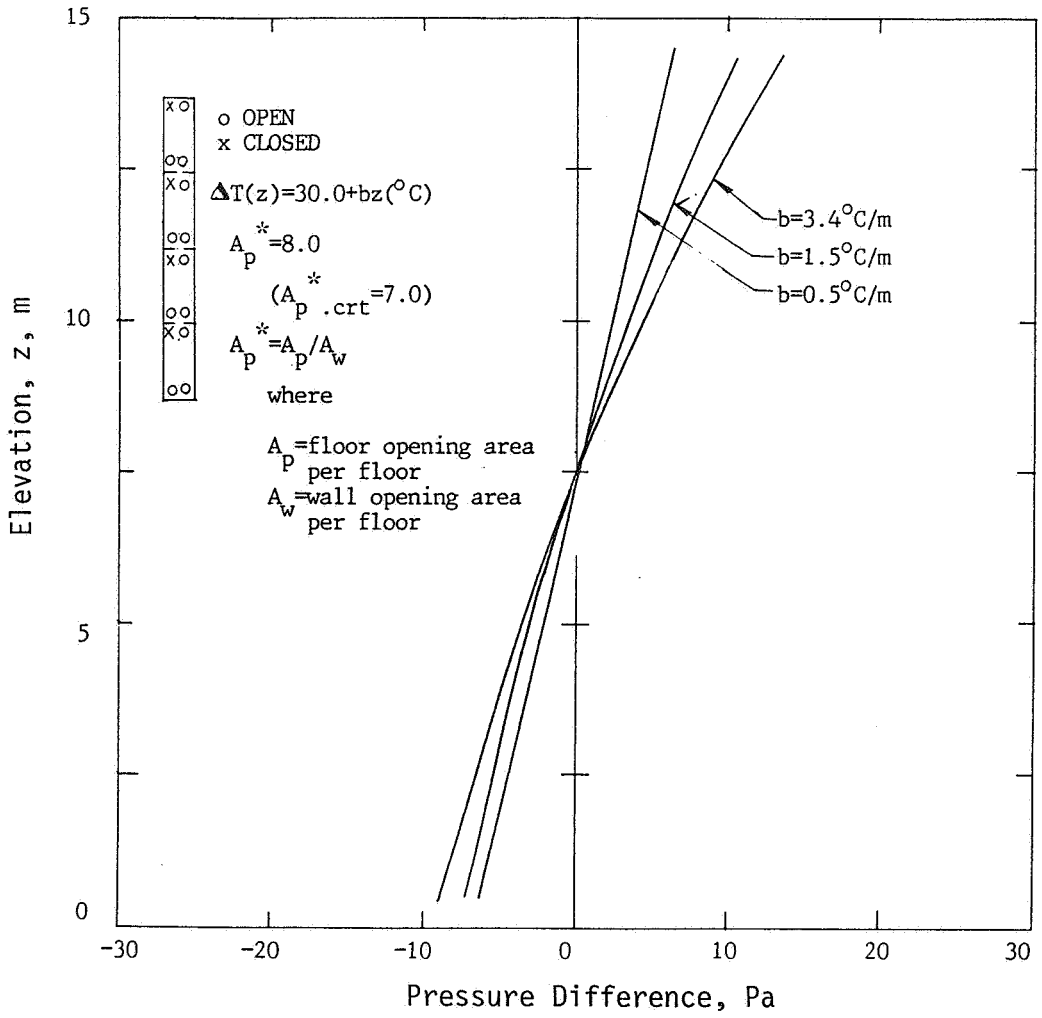

Fig. 11 Effect of "b" on Pressure Distribution; Four Floors

4.3.2 Number of Floor Openings per Floor

In actual buildings, the crack openings in the floor separations such as the cracks around elevator doors and doors to the stairways, etc., are neither situated in one place nor existing as one hole. However, in the present analysis, only one hole at the center of each floor is assumed. The possible effect of this deviation on the results should be also considered.

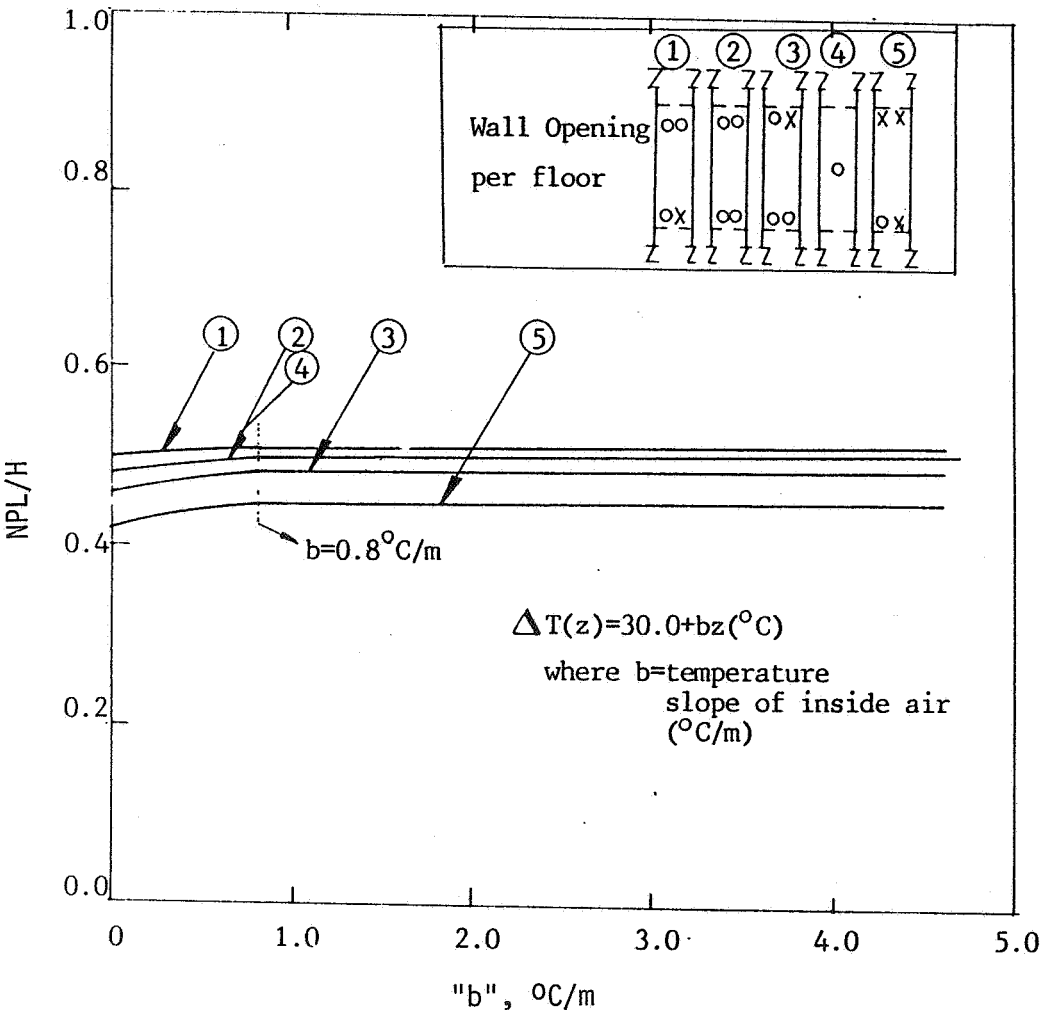

Fig. 12 Effect of "b" on NPL; Buildings with Floor Partitions

The analytical studies on the effect of dividing the floor opening area into multi-holes on the value of (Ap*)crit for the cases of two floor and four floor buildings were made. The number of floor openings per floor partition, which was assumed to have the same geometrical shape and dimension, was varied from 1 to 25, maintaining the total area constant. There was a slight increase of (Ap*)crit with the increase of the number of holes and this can be attributed to the

increase of flow resistance at the holes. The results suggest that by replacing multi-openings by a single hole, (Ap*)crit tends to be underestimated. Nevertheless, for most of the cases studied here, the calculated critical Ap* is less than the actual Ap* employed in the analysis and hence the anticipated effect on the pressure calculation should not be significant.

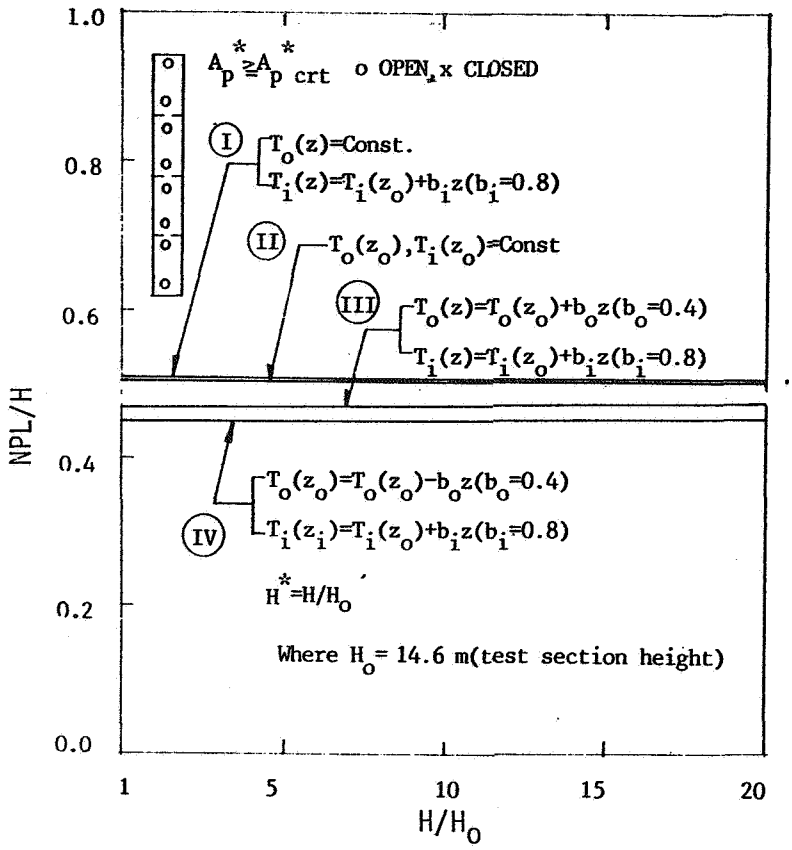

Fig. 13 Effects of "b_i" and "b_o" on NPL

5.0 CONCLUDING REMARKS

Based on the results presented above, we may conclude that the effects of non-uniform temperature distributions of inside and/or outside air along the height of buildings on the value of NPL within practical ranges of temperature differences, and on the profiles of pressure differential due to thermal effect in the actual building environment are seen to be marginal.

ACKNOWLEDGMENTS

The present study is financed by the Natural Science and Engineering Research Council of Canada, under the Strategic Grant G0411 (Energy).

REFERENCES

1. Hutchon, N.B. and Handegord, 1983. "Building Science for a Cold Climate", John Wiley and Sons.

2. McGuire, J.H. and Tamura, G.T., 1979. "The National Building Code Smoke Control Measures", Eng. Digest, 25, No. 9.

3. Lee, Y., Tanaka, H., and Shaw, C.Y., 1982. "Distribution of Wind and Temperature Induced Pressure Differences Across the Walls of a Twenty Story Compartmentalized Building", Journal of Wind Engineering and Industrial Aerodynamics, 10, pp 287-301.

4. C.Y. Shaw, 1979. "Air Tightness and Air Infiltration of School Buildings", ASHRAE Transactions, 85, pp 85-95.

5. Lee, K.H., Lee, Y., and Tanaka, H., 1986. "Thermal Effect on Pressure Distribution in Simulated High-rise Buildings: Experiment and Analysis", ASHRAE Transactions, 91, pt. 2. pp 530-544.

6. ASHRAE Handbook - 1981, Fundamentals, American Soc. of Heating, Refrigeration and Air-Conditioning Engineers.

7. Rohsenow, W.M. and Choi, H. Y., 1961. Heat, Mass and Momentum Transfer, Prentice-Hall Inc., New York, N.Y.

8. Gerald, C. F., 1984. "Applied Numerical Analysis", Chap. 2, 3rd Ed., Addison-Wesley, New York, N.Y.

9. Tanaka, H. and Lee, Y. "Stack Effect and Building Internal Pressure" (Accepted) 7th Int. Conf. on Wind Engineering, July 6/9, 1987, Aachen. (To be published as the Proceeding in the Jour. of Wind and Ind. Aerodynamics).